Chapter 4

Microbial ecology of selenium-respiring bacteria

Joshua P. Boltz and Bruce E. Rittmann

4.1 SELENIUM, SULFUR, AND NITROGEN IN A COMMON AQUATIC ENVIRONMENT

Irrigated agriculture, steam-power generation, mining, and other human activities result in water that is co-contaminated by selenium (Se), sulfur (S), and nitrogen (N) that typically exist as selenate (SeO_4^{2-}) and/or selenite ($HSeO_3^-$), sulfate (SO_4^{2-}), and nitrate (NO_3^-), respectively. Usually, their concentrations are very different, whether in irrigated agriculture run-off or in wastewater. The S-to-Se mass ratio (S:Se) is typically in the order of 1000:1 (g S:g Se) and the N-to-Se mass ratio (N:Se) is typically in the order of 50:1 (g N:g Se). The target contaminant concentrations in treated effluent also show great disparity. For example, the United States Environmental Protection Agency (EPA, 2020) requires existing steam-power-generation facilities to discharge water having less than 3 g N/m^3 and 0.029 g Se/m^3 (average daily concentrations over a consecutive 30-day period); this is a N:Se ratio ~100:1 (g N:g Se).

Selenium is among the first micro-pollutants that, according to regulation (EPA, 2020), require biological wastewater treatment and have regulated surface-water discharge standards. When the contaminated water has a pH of 6 to 8 and a temperature of 15 to 30°C, bacteria can anaerobically reduce these oxyanions at a rate that makes bioreactors an economically viable treatment alternative (Boltz &

doi: 10.2166/9781789061055_0145

Rittmann, 2019). While much is known about denitrifying heterotrophic bacteria (denoted X_H) and sulfate-reducing bacteria (denoted X_{SRB}) (see Grady *et al.*, 2011; Rittmann & McCarty, 2020), the metabolic pathways of selenium-respiring bacteria (SeRB) are not as well understood.

Selenium-respiring bacteria are phylogenetically and physiologically diverse, and they include the selenate-reducing bacterium *Thauera selenatis* (Macy *et al.*, 1993) and selenite-reducing bacterium *Bacillus selenitireducens* (Switzer Blum *et al.*, 1998). Much like denitrifying heterotrophic and sulfate-reducing bacteria, SeRB carry out respiration, synthesis, endogenous, and detoxification processes. These bacteria respire selenium, synthesize essential macro- (e.g., C and N) and micro-nutrients (e.g., Se and S), release and/or utilize their internal components through endogenous processes, and emit organic selenium compounds (e.g., selenomethionine, or SeMet) to prevent accumulating an internal selenide mass that is toxic to the bacteria. Selenate-reducing bacteria (denoted X_{SeO_4}) biologically transform selenate into selenite during respiration. Similarly, selenite-reducing bacteria (denoted X_{SeO_3}) biologically transform selenite into elemental selenium (Se^0) during respiration. Elemental selenium is a stable product that predominantly accumulates in the cells' extracellular polymeric substances (EPS). Intra-cellular Se generally exists as selenide (Se(-II)). Selenium-respiring bacteria can reduce selenium oxyanions directly to intra-cellular selenide (Se(-II)) during synthesis. Figure 4.1 illustrates the modeled processes of respiration, synthesis, and endogenous decay for selenite-reducing bacteria. The reduction of selenium oxyanions to selenide and detoxification are not modeled.

Energetically, SeRB preferentially utilize selenide as their source of Se for biomass synthesis (Eswayah *et al.*, 2016). However, Se in oxyanions also can be used for this purpose, but with an associated energy cost in the form of electron donor demand. Endogenous decay processes re-introduce selenide to the bulk of the liquid, where it can be transformed into metal selenides or re-used for biomass synthesis. In addition, selenium resulting from endogenous processes and detoxification may volatilize (see Chapter 3). Factors influencing bacterial selenium volatilization include macro-nutrient availability (particularly C and N), exposure to aerobic conditions, temperature (>30 to 35°C), pH (>8), selenium speciation, and microbial community composition (De Souza *et al.*, 2001).

This chapter begins by describing interactions among denitrifying heterotrophic bacteria, SeRB, and sulfate-reducing bacteria. Figure 4.2 illustrates that all these bacteria carry out respiration, synthesis, and endogenous decay while competing for a common electron donor and nutrient pool. The chapter then provides an energetic analysis and mathematical model of these processes, and the chapter compares model results with published data. Used together, they identify the factors controlling how SeRB occur along with denitrifying heterotrophic and sulfate-reducing bacteria in bioreactors treating Se-laden waters.

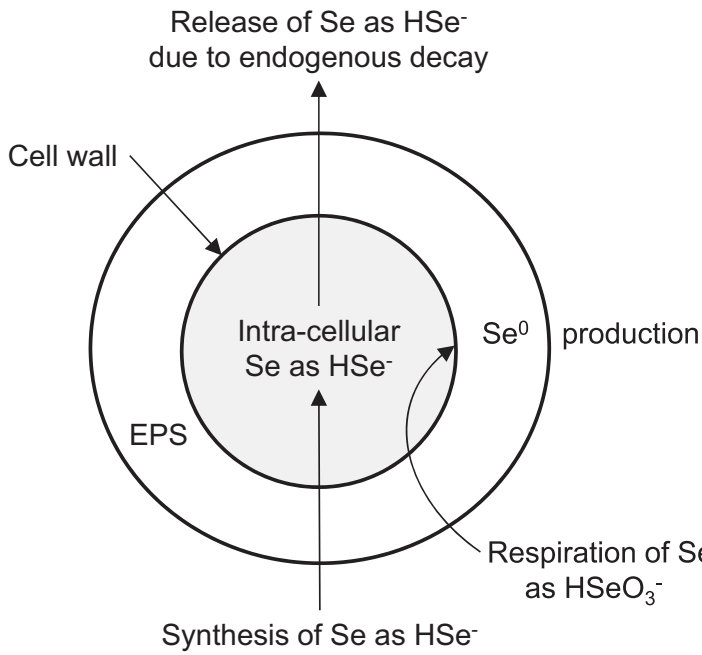

Figure 4.1 Simulated metabolic processes for selenite-reducing bacteria (X_{SeO_3}). Selenite-reducing bacteria respire selenite ($HSeO_3^-$) to produce elemental selenium (Se^0), which may accumulate inside and outside the cell wall. These bacteria synthesize selenium as selenide (HSe^-). An intra-cellular pool of nutrients, including HSe^-, exists inside a cell wall. Extracellular polymeric substances (EPS) exist outside the cell wall.

4.2 SUBSTRATE PARTITIONING, ENERGETICS, AND BIOMASS YIELD

Microorganisms carry out oxidation-reduction reactions to obtain energy for synthesis and cell maintenance (Rittmann & McCarty, 2020). The amount of energy released per electron equivalent depends on the reaction. Consequently, the amount of synthesis resulting from an equivalent of electron donor oxidized also depends on the reaction. When microorganisms utilize an electron donor, they transfer a portion of their electrons to the electron acceptor (fraction f_e^0) to supply the energy required for converting the remaining electrons (fraction f_s^0) into microbial cells; the fractions add to one, or $f_e^0 + f_s^0 = 1$. We apply a thermodynamic electron-equivalent model (McCarty, 2007; Rittmann & McCarty, 2020) to relate synthesis and reaction energetics. We begin with the four electron acceptors used in respiration, consider a common electron donor, develop the energy reactions, and then factor in biomass synthesis.

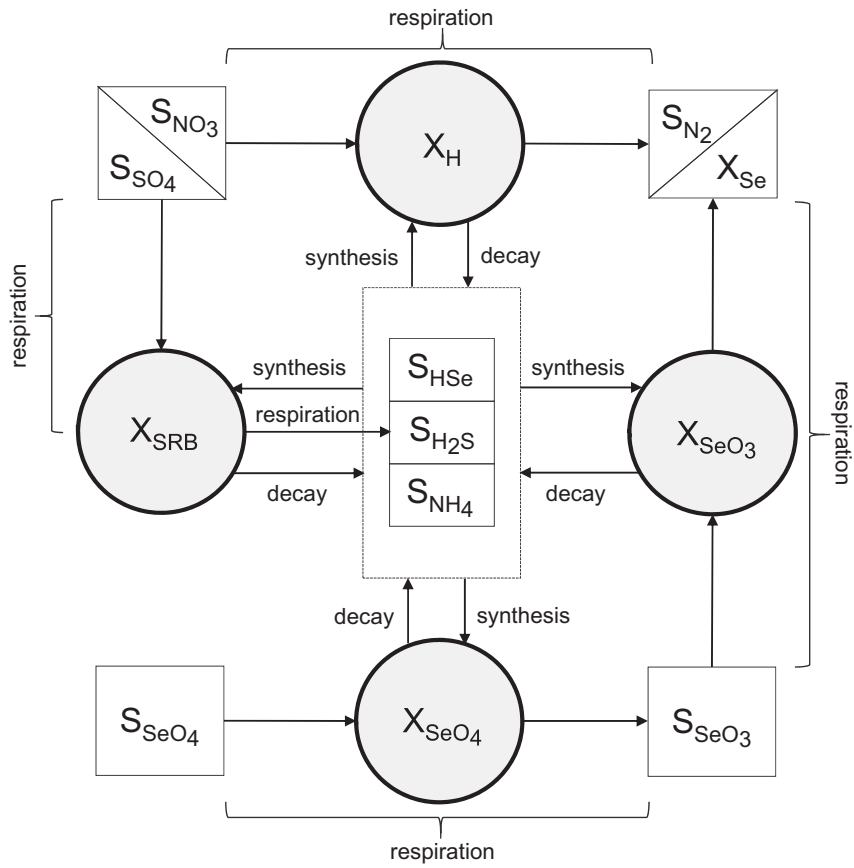

Figure 4.2 Interactions among denitrifying heterotrophic bacteria (X_H), selenate-reducing bacteria (X_{SeO_4}), selenite-reducing bacteria (X_{SeO_3}), and sulfate-reducing bacteria (X_{SRB}) undergoing respiration, synthesis, and endogenous decay. Symbols: nitrate (S_{NO_3}), di-nitrogen (S_{N_2}), ammonium (S_{NH_4}), selenate (S_{SeO_4}), selenite (S_{SeO_3}), elemental selenium (X_{Se}), selenide (S_{HSe}), sulfate (S_{SO_4}), and hydrogen sulfide (S_{H_2S}).

4.2.1 Electron-acceptor reductions

Equation (4.1) is the half reaction for nitrate reduction to di-nitrogen (N_2) and its free energy (Grady *et al.*, 2011; Rittmann & McCarty, 2020):

$$\frac{1}{5}NO_3^- + \frac{6}{5}H^+ + e^- \rightarrow \frac{1}{10}N_2 + \frac{3}{5}H_2O \quad \Delta G^{0'}_{EA} = -72.2\frac{kJ}{e^- eq_{EA}} \tag{4.1}$$

Equation (4.2) is the half reaction for selenate reduction to selenite and its free energy (Olin *et al.*, 2020; PSI, 2007):

$$\frac{1}{2}SeO_4^{2-} + \frac{3}{2}H^+ + e^- \rightarrow \frac{1}{2}HSeO_3^- + \frac{1}{2}H_2O \qquad \Delta G_{EA}^{0'} = -43.9\frac{kJ}{e^- eq_{EA}} \tag{4.2}$$

Equation (4.3) is the half reaction for selenite reduction to elemental selenium and its free energy (Olin *et al.*, 2020; PSI, 2007):

$$\frac{1}{4}HSeO_3^- + \frac{5}{4}H^+ + e^- \rightarrow \frac{1}{4}Se^0 + \frac{3}{4}H_2O \qquad \Delta G_{EA}^{0'} = -25.4\frac{kJ}{e^- eq_{EA}} \tag{4.3}$$

Finally, Equation (4.4) is the half reaction for sulfate reduction to hydrogen sulfide (H_2S) and its free energy (Grady *et al.*, 2011; Rittmann & McCarty, 2020):

$$\frac{1}{8}SO_4^{2-} + \frac{5}{4}H^+ + e^- \rightarrow \frac{1}{8}H_2S + \frac{1}{2}H_2O \qquad \Delta G_{EA}^{0'} = +20.1\frac{kJ}{e^- eq_{EA}} \tag{4.4}$$

Standard free energies have been adjusted to pH = 7 (i.e., $\Delta G^{0'}$) for all reactions, following Rittmann and McCarty (2020).

4.2.2 Oxidation of a common electron donor

Acetate (CH_3COO^-) is the common electron donor for all electron acceptors. Equation (4.5) is the half reaction for acetate reduction and its free energy (Rittmann & McCarty, 2020):

$$\frac{1}{8}CH_3COO^- + \frac{1}{8}H_2O \rightarrow \frac{1}{8}CO_2 + \frac{1}{8}HCO_3^- + H^+ + e^-$$
$$\Delta G_{ED}^{0'} = +27.4\frac{kJ}{e^- eq_{ED}} \tag{4.5}$$

4.2.3 Energy reactions

Equations (4.6) through (4.9) are the energy reactions for each of the four electron acceptors when acetate is the common electron donor. Also shown are the free energy values for each energy reaction ($\Delta G^{0'}$) kJ/e^-eq.

$$\frac{1}{8}CH_3COO^- + \frac{1}{5}NO_3^- + \frac{1}{5}H^+ \rightarrow \frac{1}{8}CO_2 + \frac{1}{10}N_2 + \frac{1}{8}HCO_3^- + \frac{19}{40}H_2O$$
$$\Delta G_{ED}^{0'} = -99.6\frac{kJ}{e^- eq_{ED}} \tag{4.6}$$

$$\frac{1}{8}CH_3COO^- + \frac{1}{2}SeO_4^{2-} + \frac{1}{2}H^+ \rightarrow \frac{1}{8}CO_2 + \frac{1}{2}HSeO_3^- + \frac{1}{8}HCO_3^- + \frac{3}{8}H_2O$$
$$\Delta G_{ED}^{0'} = -71.3 \frac{kJ}{e^- eq_{ED}} \quad (4.7)$$

$$\frac{1}{8}CH_3COO^- + \frac{1}{4}HSeO_3^- + \frac{1}{4}H^+ \rightarrow \frac{1}{8}CO_2 + \frac{1}{4}Se^0 + \frac{1}{8}HCO_3^- + \frac{5}{8}H_2O$$
$$\Delta G_{ED}^{0'} = -49.8 \frac{kJ}{e^- eq_{ED}} \quad (4.8)$$

$$\frac{1}{8}CH_3COO^- + \frac{1}{8}SO_4^{2-} + \frac{1}{4}H^+ \rightarrow \frac{1}{8}CO_2 + \frac{1}{8}H_2S + \frac{1}{8}HCO_3^- + \frac{3}{8}H_2O$$
$$\Delta G_{ED}^{0'} = -7.3 \frac{kJ}{e^- eq_{ED}} \quad (4.9)$$

Equations (4.6) through (4.9) show significant differences in $\Delta G^{0'}$ values, which vary from -99.6 to -7.3 kJ/e$^-$eq$_{ED}$. These differences stem from the free energies for the electron acceptors (Equations (4.1) through (4.4)), which range from -72.2 to $+20.1$ kJ/e$^-$eq$_{EA}$. These free-energy differences have strong implications on the competitiveness of bacteria carrying out different respirations. Denitrifying heterotrophic bacteria have a significant energy advantage over the other bacteria considered here, while sulfate-reducing bacteria have a significant energy disadvantage. Noteworthy is that the conversion of selenate into selenite (Equation (4.2)) has a $\Delta G^{0'}$ value that is more negative by 18.5 kJ/e$^-_{ED}$ when compared with the conversion of selenite into elemental selenium (Equation (4.3)). The more negative free energy indicates a competitive advantage for selenate-reducing bacteria when they are competing with selenite-reducing bacteria for a common electron donor.

4.2.4 Considering biomass synthesis

Rittmann and McCarty (2020) presented a method for quantifying biomass synthesis based on balancing energy gained in the energy reactions (i.e., Equations (4.6) through (4.9)) with the demand that is associated with synthesizing biomass from available forms of the essential macro-nutrients, of which C and N are dominating. Because all of the bacteria in our analysis have the same sources of C (acetate) and N (ammonium), the energy associated with synthesis is the same in all cases: 37.2 kJ/e$^-$ eq$_X$. This value is combined with ΔG_r to compute A, which is the ratio of electron equivalents used for the energy reaction to the electron equivalents used for biomass

synthesis (from the energy balance):

$$A = \frac{-37.2}{\varepsilon \cdot \Delta G_r} \tag{4.10}$$

Here, ε is the energy-transfer efficiency, which we take as 0.68, a value within the typical range of 0.55 to 0.70 (Rittmann & McCarty, 2020). The ΔG_r values are taken from Equations (4.6) through (4.9).

Then, f_s^0 can be calculated by:

$$f_s^0 = \frac{1}{1 + A} \tag{4.11}$$

Since one electron equivalent equals 8 g O_2, the true yield for any of the bacteria (Y_k) can be calculated by:

$$Y_k = \frac{f_s^0 \cdot M_c}{8 \cdot n_e} \cdot 1.42 \frac{\text{g COD}_\text{X}}{\text{g VSS}} \tag{4.12}$$

Here, M_c is the molecular weight of bacterial cells (113 g volatile suspended solids (VSS)/mol VSS), n_e is the number of electron equivalents in an empirical mole of bacterial cells, i.e., 20 e^-eq_{VSS}/mol VSS when ammonium is the N source, and 1.42 is a conversion factor for biomass chemical oxygen demand (COD) and VSS (Rittmann & McCarty, 2020).

The maximum specific rate of electron-donor utilization, or q_k, can be calculated by:

$$q_k = \frac{8}{f_e^0} \cdot \frac{1}{1.42} \frac{\text{g VSS}}{\text{g COD}_\text{X}} \tag{4.13}$$

Here, q_k has units $\left(\frac{\text{g COD}_\text{ED}}{\text{g COD}_\text{X} \cdot \text{d}}\right)$. The maximum specific growth rate of any biomass k ($\mu_{\max,k}$) can be calculated by:

$$\mu_{\max,k} = Y_k \cdot q_k \tag{4.14}$$

Table 4.1 summarizes the results of this analysis for the respirations described by Equations (4.6) through (4.9). Striking about Table 4.1 are the significant differences in Y_k and $\mu_{\max,k}$ values. Reflecting the trends in the $\Delta G^{0'}$ values associated with Equations (4.6) through (4.9), the Y_k and $\mu_{\max,k}$ values indicate a clear advantage for denitrifying heterotrophic bacteria when compared with the other bacteria considered. The advantages indicated by both of these parameters suggest a kinetic hierarchy for the specific growth rate: denitrifying heterotrophic bacteria > selenate-reducing bacteria > selenite-reducing bacteria > sulfate-reducing bacteria. The differences among Y_k and $\mu_{\max,k}$ are substantial enough to suggest that it is possible to favor or suppress the accumulation of different bacterial types in a well-designed and operated bioreactor.

Table 4.1 Stoichiometry and energetics for the four respiration reactions.

Electron Donor (ED)	Electron Acceptor (EA)	Reduced Product	Energy Equivalents Required for Cell Production, A $\left(\frac{e^- eq_s}{e^- eq_{ED}}\right)$	Fraction of Electrons Required for Cell Synthesis, f_s^0 $\left(\frac{e^- eq_X}{e^- eq_{ED}}\right)$	Fraction of Electrons Required for Energy Production, f_e^0 $\left(\frac{e^- eq_{EA}}{e^- eq_{ED}}\right)$	Biomass Yield, Y $\left(\frac{g_{COD_X}}{g_{COD_{ED}}}\right)$	Maximum Specific Rate of Substrate Utilization, q_{max} $\left(\frac{g_{COD_{ED}}}{g_{COD_X} \cdot d}\right)$	Maximum Specific Growth Rate of Biomass, μ_{max} $\left(\frac{1}{d}\right)$
Acetate	NO_3^-	N_2	0.55	0.65	0.35	0.65	15.9	10.3
Acetate	SeO_4^{2-}	$HSeO_3^-$	0.77	0.57	0.43	0.57	13.0	7.4
Acetate	$HSeO_3^-$	Se^0	1.04	0.49	0.51	0.49	11.1	5.5
Acetate	SO_4^{2-}	H_2S	7.49	0.12	0.88	0.12	6.4	0.8

4.3 MATHEMATICAL MODEL OF DENITRIFYING HETEROTROPHIC BACTERIA, SELENIUM-RESPIRING BACTERIA, AND SULFATE-REDUCING BACTERIA

The mathematical model presented in this chapter explicitly simulates electron-donor oxidation, electron-acceptor respiration, biomass synthesis, macro- and micro-nutrient assimilation for synthesis, and endogenous decay for denitrifying heterotrophic bacteria, selenate-reducing bacteria, selenite-reducing bacteria, and sulfate-reducing bacteria. These bacteria compete for essential nutrients that include the electron donor acetate (denoted S_{VFA}), macro-nutrient ammonium (denoted S_{NHx}), and the micro-nutrients hydrogen sulfide (denoted S_{H_2S}) and selenide (denoted S_{HSe}). Grady *et al.* (2011) and Rittmann and McCarty (2020) present comprehensive discussions about biological process models and their applications.

Table 4.2 presents the process, kinetic, and stoichiometric matrix for denitrifying heterotrophic bacteria. Simulated processes include the anaerobic biological transformation of nitrate (denoted S_{NO_3}) to di-nitrogen (denoted S_{N_2}) and anaerobic endogenous decay. Table 4.3 presents the process, kinetic, and stoichiometric matrix for selenate-reducing bacteria. Simulated processes include the anaerobic biological transformation of selenate (denoted S_{SeO_4}) to selenite (denoted S_{SeO_3}) and anaerobic endogenous decay. Table 4.4 presents the process, kinetic, and stoichiometric matrix for selenite-reducing bacteria. Simulated processes include the anaerobic biological transformation of selenite to elemental selenium (denoted X_{Se}) and anaerobic endogenous decay. Finally, Table 4.5 presents the process, kinetic, and stoichiometric matrix for sulfate-reducing bacteria. Simulated processes include the anaerobic biological transformation of sulfate (denoted S_{SO_4}) to hydrogen sulfide and anaerobic endogenous decay.

Kinetic expressions for each of the simulated processes are listed in Table 4.6. The rates of electron-donor oxidation, electron-acceptor reduction, biomass synthesis, and macro- and micro-nutrient assimilation are represented as the product of a maximum specific growth rate of biomass ($\mu_{\max,k}$), Monod-type hyperbolic functions for each potentially rate-limiting substrate i $\left(\frac{S_i}{S_i + K_i}\right)$, and the concentration of biomass k (X_k). The rate expressions may include one or more functions that inhibit bacterial growth when other electron acceptors are present in sufficient quantity $\left(\frac{K_i}{S_i + K_i}\right)$. For example, a sufficient nitrate concentration will inhibit selenate, selenite, and sulfate reductions. Endogenous decay kinetics are simulated as first-order expressions that multiply a biomass decay rate (b_k) and the concentration of biomass k (X_k).

Table 4.7 defines kinetic parameters, and Table 4.8 defines conversion factors and stoichiometric parameters for each of the modeled bacteria. A parameter of

Table 4.2 Process, kinetic, and stoichiometric matrix for denitrifying heterotrophic bacteria (X_H).

j	Name	S_{VFA}	S_{NHx}	S_{N_2}	S_{NO_3}	S_{H_2S}	S_{HSe}	X_H	X_B	X_I	Rate
1	Anaerobic growth of X_H on S_{VFA} ($S_{NO_3} \rightarrow S_{N_2}$)	$-\frac{1}{Y_H}$	$-i_{N,BM}$	$\frac{1-Y_H}{Y_H \cdot \frac{40}{14}}$	$-\frac{1-Y_H}{Y_H \cdot \frac{40}{14}}$	$-i_{S,BM}$	$-i_{Se,BM}$	1			R1
2	Anaerobic endogenous decay of X_H		$i_{N,2}$			$i_{S,2}$	$i_{Se,2}$	−1	$1-f_{I,H}$	$f_{I,H}$	R2
	Composition:										
	COD	1	0	$-\frac{24}{14}$	$-\frac{64}{14}$	0	0	1	1	1	
	N	0	1	1	1	0	0	$i_{N,BM}$	$i_{N,XB}$	$i_{N,I}$	
	S	0	0	0	0	1	0	$i_{S,BM}$	$i_{S,XB}$	$i_{S,I}$	
	Se	0	0	0	0	0	1	$i_{Se,BM}$	$i_{Se,XB}$	$i_{Se,I}$	

$i_{N,2} = i_{N,BM} - i_{N,I} \cdot f_{I,H} - i_{N,XB} \cdot (1 - f_{I,H})$
$i_{S,2} = i_{S,BM} - i_{S,I} \cdot f_{I,H} - i_{S,XB} \cdot (1 - f_{I,H})$
$i_{Se,2} = i_{Se,BM} - i_{Se,I} \cdot f_{I,H} - i_{Se,XB} \cdot (1 - f_{I,H})$

Table 4.3 Process, kinetic, and stoichiometric matrix for selenate-reducing bacteria (X_{SeO_4}).

j	Name	S_{VFA}	S_{NHx}	S_{H_2S}	S_{HSe}	S_{SeO_3}	S_{SeO_4}	X_{SeO_4}	X_B	X_I	Rate
3	Anaerobic growth of X_{SeO_4} on S_{VFA} ($S_{SeO_4} \rightarrow S_{SeO_3}$)	$-\frac{1}{Y_{SeO_4}}$	$-i_{N,BM}$	$-i_{S,BM}$	$-i_{Se,BM}$	$\frac{1-Y_{SeO_4}}{Y_{SeO_4}\cdot\frac{16}{79}}$	$-\frac{1-Y_{SeO_4}}{Y_{SeO_4}\cdot\frac{16}{79}}$	1			R3
4	Anaerobic endogenous decay of X_{SeO_4}		$i_{N,4}$	$i_{S,4}$	$i_{Se,4}$			−1	$1-f_{I,SeO_4}$	f_{I,SeO_4}	R4
	Composition:										
	COD	1	0	0	0	$-\frac{48}{79}$	$-\frac{64}{79}$	1	1	1	
	N	0	1	0	0	0	0	$i_{N,BM}$	$i_{N,XB}$	$i_{N,I}$	
	S	0	0	1	0	0	0	$i_{S,BM}$	$i_{S,XB}$	$i_{S,I}$	
	Se	0	0	0	1	1	1	$i_{Se,BM}$	$i_{Se,XB}$	$i_{Se,I}$	

$i_{N,4} = i_{N,BM} - i_{N,I}\cdot f_{I,SeO_4} - i_{N,XB}\cdot(1-f_{I,SeO_4})$
$i_{S,4} = i_{S,BM} - i_{S,I}\cdot f_{I,SeO_4} - i_{S,XB}\cdot(1-f_{I,SeO_4})$
$i_{Se,4} = i_{Se,BM} - i_{HSe,I}\cdot f_{I,SeO_4} - i_{Se,XB}\cdot(1-f_{I,SeO_4})$

Table 4.4 Process, kinetic, and stoichiometric matrix for selenite-reducing bacteria (X_{SeO_3}).

j	Name	S_{VFA}	S_{NHx}	S_{H_2S}	S_{HSe}	X_{Se}	S_{SeO_3}	X_{SeO_3}	X_B	X_I	Rate
5	Anaerobic growth of X_{SeO_3} on S_{VFA} ($S_{SeO_3} \rightarrow X_{Se}$)	$-\frac{1}{Y_{SeO_3}}$	$-i_{N,BM}$	$-i_{S,BM}$	$-i_{Se,BM}$	$\frac{1-Y_{SeO_3}}{Y_{SeO_3}\cdot\frac{32}{79}}$	$-\frac{1-Y_{SeO_3}}{Y_{SeO_4}\cdot\frac{32}{79}}$	1			R5
6	Anaerobic endogenous decay of X_{SeO_3}		$i_{N,6}$	$i_{S,6}$	$i_{Se,6}$			−1	$1-f_{I,SeO_3}$	f_{I,SeO_3}	R6
	Composition:										
	COD	1	0	0	0	$-\frac{16}{79}$	$-\frac{48}{79}$	1	1	1	
	N	0	1	0	0	0	0	$i_{N,BM}$	$i_{N,XB}$	$i_{N,I}$	
	S	0	0	1	0	0	0	$i_{S,BM}$	$i_{S,XB}$	$i_{S,I}$	
	Se	0	0	0	1	1	1	$i_{Se,BM}$	$i_{Se,XB}$	$i_{Se,I}$	

$i_{N,6} = i_{N,BM} - i_{N,I}\cdot f_{I,SeO_3} - i_{N,XB}\cdot(1-f_{I,SeO_3})$
$i_{S,6} = i_{S,BM} - i_{S,I}\cdot f_{I,SeO_3} - i_{S,XB}\cdot(1-f_{I,SeO_3})$
$i_{Se,6} = i_{Se,BM} - i_{Se,I}\cdot f_{I,SeO_3} - i_{Se,XB}\cdot(1-f_{I,SeO_3})$

Table 4.5 Process, kinetic, and stoichiometric matrix for sulfate-reducing bacteria (X_{SRB}).

j	Name	S_{VFA}	S_{NHx}	S_{H_2S}	S_{SO_4}	S_{HSe}	X_{SRB}	X_B	X_I	Rate
7	Anaerobic growth of X_{SRB} on S_{VFA} ($S_{SO_4} \rightarrow S_{H_2S}$)	$-\frac{1}{Y_{SRB}}$	$-i_{N,BM}$	$\frac{1-Y_{SRB}}{Y_{SRB}\cdot\frac{64}{32}}-i_{S,BM}$	$-\frac{1-Y_{SRB}}{Y_{SRB}\cdot\frac{64}{32}}$	$-i_{Se,BM}$	1			R7
8	Anaerobic endogenous decay of X_{SRB}		$i_{N,8}$	$i_{S,8}$		$i_{Se,8}$	−1	$1-f_{I,SRB}$	$f_{I,SRB}$	R8
	Composition:									
	COD	1	0	0	$-\frac{64}{32}$	0	1	1	1	
	N	0	1	0	1	0	$i_{N,BM}$	$i_{N,XB}$	$i_{N,I}$	
	S	0	0	1	0	0	$i_{S,BM}$	$i_{S,XB}$	$i_{S,I}$	
	Se	0	0	0	0	1	$i_{Se,BM}$	$i_{Se,XB}$	$i_{Se,I}$	

$i_{N,8} = i_{N,BM} - i_{N,I}\cdot f_{I,SRB} - i_{N,XB}\cdot(1-f_{I,SRB})$
$i_{S,8} = i_{S,BM} - i_{S,I}\cdot f_{I,SRB} - i_{S,XB}\cdot(1-f_{I,SRB})$
$i_{Se,8} = i_{Se,BM} - i_{Se,I}\cdot f_{I,SRB} - i_{Se,XB}\cdot(1-f_{I,SRB})$

Table 4.6 Process rate equations for denitrifying heterotrophic bacteria (X_H), selenate-reducing bacteria (X_{SeO_4}), selenite-reducing bacteria (X_{SeO_3}), and sulfate-reducing bacteria (X_{SRB}) growth and endogenous decay.

	Name	Process Rate Equation ($g/m^3 \cdot d$)
R1	Anaerobic growth of X_H on S_{VFA} ($S_{NO_3} \rightarrow S_{N_2}$)	$\mu_{max,H} \cdot \frac{S_{VFA}}{K_{VFA,H} + S_{VFA}} \cdot \frac{S_{NO_3}}{K_{NO_3,H} + S_{NO_3}} \cdot \frac{S_{NHx}}{K_{NHx,H} + S_{NHx}} \cdot \frac{S_{H_2S}}{K_{H_2S,H} + S_{H_2S}} \cdot \frac{S_{HSe}}{K_{HSe,H} + S_{Hse}} \cdot X_H$
R2	Anaerobic endogenous decay of X_H	$b_H \cdot X_H$
R3	Anaerobic growth of X_{SeO_4} on S_{VFA} ($S_{SeO_4} \rightarrow S_{SeO_3}$)	$\mu_{max,SeO_4} \cdot \frac{K_{NO_3,SeO_4}}{K_{NO_3,SeO_4} + S_{NO_3}} \cdot \frac{S_{VFA}}{K_{VFA,SeO_4} + S_{VFA}} \cdot \frac{S_{SeO_4}}{K_{SeO_4,SeO_4} + S_{SeO_4}} \cdot \frac{S_{NHx}}{K_{NHx,SeO_4} + S_{NHx}} \cdot \frac{S_{H_2S}}{K_{H_2S,SeO_4} + S_{H_2S}} \cdot \frac{S_{HSe}}{K_{HSe,SeO_4} + S_{Hse}} \cdot X_{SeO_4}$
R4	Anaerobic endogenous decay of X_{SeO_4}	$b_{SeO_4} \cdot X_{SeO_4}$
R5	Anaerobic growth of X_{SeO_3} on S_{VFA} ($S_{SeO_3} \rightarrow X_{Se}$)	$\mu_{max,SeO_3} \cdot \frac{K_{NO_3,SeO_3}}{K_{NO_3,SeO_3} + S_{NO_3}} \cdot \frac{K_{SeO_4,SeO_3}}{K_{SeO_4,SeO_3} + S_{SeO_4}} \cdot \frac{S_{VFA}}{K_{VFA,SeO_3} + S_{VFA}} \cdot \frac{S_{SeO_3}}{K_{SeO_3,SeO_3} + S_{SeO_3}} \cdot \frac{S_{NHx}}{K_{NHx,SeO_3} + S_{NHx}} \cdot \frac{S_{H_2S}}{K_{H_2S,SeO_3} + S_{H_2S}} \cdot \frac{S_{HSe}}{K_{HSe,SeO_3} + S_{Hse}} X_{SeO_3}$
R6	Anaerobic endogenous decay of X_{SeO_3}	$b_{SeO_3} \cdot X_{SeO_3}$
R7	Anaerobic growth of X_{SRB} on S_{VFA} ($S_{SO_4} \rightarrow S_{H_2S}$)	$\mu_{max,SRB} \cdot \frac{K_{NO_3,SRB}}{K_{NO_3,SRB} + S_{NO_3}} \cdot \frac{K_{SeO_4,SRB}}{K_{SeO_4,SRB} + S_{SeO_4}} \cdot \frac{K_{SeO_3,SRB}}{K_{SeO_3,SRB} + S_{SeO_3}} \cdot \frac{S_{VFA}}{K_{VFA,SRB} + S_{VFA}} \cdot \frac{S_{SO_4}}{K_{SO_4,SRB} + S_{SO_4}} \cdot \frac{S_{NHx}}{K_{NHx,SRB} + S_{NHx}} \cdot \frac{S_{H_2S}}{K_{H_2S,SRB} + S_{H_2S}} \cdot \frac{S_{HSe}}{K_{HSe,SRB} + S_{Hse}} \cdot X_{SRB}$
R8	Anaerobic endogenous decay of X_{SRB}	$b_{SRB} \cdot X_{SRB}$

Table 4.7 Kinetic parameters for denitrifying heterotrophic bacteria (X_H), selenate-reducing bacteria (X_{SeO_4}), selenite-reducing bacteria (X_{SeO_3}), and sulfate-reducing bacteria (X_{SRB}) growth and endogenous decay.

Symbol	Description	Value	Unit
Denitrifying heterotrophic bacteria (X_H):			
$\mu_{max,H}$	Maximum growth rate of X_H on S_{VFA}	10.30	1/d
b_H	Anaerobic endogenous decay rate, X_H	0.40	1/d
$K_{VFA,H}$	Half-saturation concentration, S_{VFA}	4.00	g COD_S/m^3
$K_{NO_3,H}$	Half-saturation concentration, S_{NO_3}	0.50	g N/m^3
$K_{NHx,H}$	Half-saturation concentration, S_{NHx}	0.05	g N/m^3
$K_{H_2S,H}$	Half-saturation concentration, S_{H_2S}	0.01	g S/m^3
$K_{HSe,H}$	Half-saturation concentration, S_{HSe}	0.001	g Se/m^3
Selenate-reducing bacteria (X_{SeO_4}):			
μ_{max,SeO_4}	Maximum growth rate of X_{SeO_4} on S_{VFA}	7.40	1/d
b_{SeO_4}	Anaerobic endogenous decay rate, X_{SeO_4}	0.29	1/d
K_{VFA,SeO_4}	Half-saturation concentration, S_{VFA}	4.00	g COD_S/m^3
K_{NO_3,SeO_4}	Inhibition concentration, S_{NO_3}	0.20	g N/m^3
K_{NHx,SeO_4}	Half-saturation concentration, S_{NHx}	0.05	g N/m^3
K_{H_2S,SeO_4}	Half-saturation concentration, S_{H_2S}	0.01	g S/m^3
K_{SeO_4,SeO_4}	Half-saturation concentration, S_{SeO_4}	0.20 *	g Se/m^3
K_{HSe,SeO_4}	Half-saturation concentration, S_{HSe}	0.001	g Se/m^3
Selenite-reducing bacteria (X_{SeO_3}):			
μ_{max,SeO_3}	Maximum growth rate of X_{SeO_3} on S_{VFA}	5.50	1/d
b_{SeO_3}	Anaerobic endogenous decay rate, X_{SeO_3}	0.21	1/d
K_{VFA,SeO_3}	Half-saturation concentration, S_{VFA}	4.00	g COD_S/m^3
K_{NO3,SeO_3}	Inhibition concentration, S_{NO_3}	0.20	g N/m^3
K_{NHx,SeO_3}	Half-saturation concentration, S_{NHx}	0.05	g N/m^3
K_{H_2S,SeO_3}	Half-saturation concentration, S_{H_2S}	0.01	g S/m^3
K_{SeO_3,SeO_3}	Half-saturation concentration, S_{SeO_3}	0.20 *	g Se/m^3
K_{HSe,SeO_3}	Half-saturation concentration, S_{HSe}	0.001	g Se/m^3
K_{SeO_4,SeO_3}	Inhibition concentration, S_{SeO_4}	0.02	g Se/m^3
Sulfate-reducing bacteria (X_{SRB}):			
$\mu_{max,SRB}$	Maximum growth rate of X_{SRB} on S_{VFA}	0.80	1/d
b_{SRB}	Anaerobic endogenous decay rate, X_{SRB}	0.03	1/d
$K_{VFA,SRB}$	Half-saturation concentration, S_{VFA}	4.00	g COD_S/m^3
$K_{NO_3,SRB}$	Inhibition concentration, S_{NO_3}	0.20	g N/m^3

(*Continued*)

Table 4.7 Kinetic parameters for denitrifying heterotrophic bacteria (X_H), selenate-reducing bacteria (X_{SeO_4}), selenite-reducing bacteria (X_{SeO_3}), and sulfate-reducing bacteria (X_{SRB}) growth and endogenous decay (*Continued*).

Symbol	Description	Value	Unit
$K_{NHx,SRB}$	Half-saturation concentration, S_{NHx}	0.05	g N/m^3
$K_{SO_4,SRB}$	Half-saturation concentration, S_{SO_4}	0.20	g S/m^3
$K_{H_2S,SRB}$	Half-saturation concentration, S_{H_2S}	0.01	g S/m^3
$K_{HSe,SRB}$	Half-saturation concentration, S_{HSe}	0.001	g Se/m^3
$K_{SeO_4,SRB}$	Inhibition concentration, S_{SeO_4}	0.02	g Se/m^3
$K_{SeO_3,SRB}$	Inhibition concentration, S_{SeO_3}	0.02	g Se/m^3

* If $S_{SeOx} > 1$, then $K_{SeOx,SeOx} = 0.04$ ($S_{SeOx,INF}$); $S_{SeOx} = S_{SeO_4} + S_{SeO_3}$

particular interest is the mass of selenium consumed for biomass synthesis ($i_{Se,BM}$ = 0.0002 g Se/g COD_X). Selenite-reducing bacteria have an intra-cellular selenium content that depends on their activity: it approaches 0.04 g Se/g COD_X when they are respiring selenium (Tan, 2018). Mörschbächer *et al.* (2018) reported that the respiration-associated content of selenium in selenite-reducing bacteria is 0.01 to 0.02 g Se/g COD_X, but also demonstrated that selenite-reducing bacteria have an intra-cellular selenium content of 0.0001 to 0.0002 g Se/g COD_X prior to respiring selenite and accumulating elemental selenium. De Souza *et al.* (2001) claimed 6% Se for selenate reduction by a bacterial consortium in an aerobic, hypersaline pond. Selenium-oxyanion reduction predominantly takes place under anaerobic conditions; therefore, non-selenium respiring bacteria reduced selenate to acquire selenium for cell synthesis. The researchers also reported that the cellular selenium content resulting from assimilation was 0.0001 to 0.0003 g Se/g COD_X. The amount of selenium is less than the amount of nitrogen required for assimilation ($i_{N,BM} = 0.07$ g N/g COD_X). Comparing the mass of nitrogen and selenium consumed for biomass synthesis, bacteria require approximately 350 times more nitrogen than selenium.

Because the mass of selenium that needs to be removed from wastewater is typically significantly less than the mass of nitrogen (recall the first paragraph), it is reasonable to consider whether or not significant selenium removal can be achieved by selenium oxyanion reduction for selenium assimilation into denitrifying heterotrophic bacteria. We consider denitrifying heterotrophic bacteria ($Y_H = 0.65$ g COD_x/g COD_{ED}) in a bioreactor treating wastewater containing 50 g N/m^3 as nitrate. Since denitrification requires 2.86 g COD_{ED}/g N, [50 g N/m^3 · 2.86 g COD_{ED}/g N · 0.65 g COD_X/g COD_{ED} · 0.0002 g Se/g COD_X] = 0.019 g Se/m^3 is assimilated by synthesis of denitrifying heterotrophic bacteria when all of the influent nitrate is respired. If the influent selenium

Table 4.8 Conversion factors and stoichiometric parameters.

Symbol	Description	Value	Unit
Nitrogen:			
$i_{N,BM}$	Nitrogen content of biomass: X_H, X_{SeO_4}, X_{SeO_3}, X_{SRB}	0.07	g N/g COD_X
$i_{N,XB}$	Nitrogen content of slowly biodegradable COD, X_B	0.04	g N/g COD_X
$i_{N,I}$	Nitrogen content of particulate inert COD, X_I	0.03	g N/g COD_X
Selenium:			
$i_{Se,BM}$	Selenium content of biomass: X_H, X_{SeO_4}, X_{SeO_3}, X_{SRB}	0.0002	g Se/g COD_X
$i_{Se,XB}$	Selenium content of particulate COD, X_B	0.0000	g Se/g COD_X
$i_{Se,I}$	Selenium content of particulate inert COD, X_I	0.0000	g Se/g COD_X
Sulfur:			
$i_{S,BM}$	Sulfur content of biomass: X_H, X_{SeO_4}, X_{SeO_3}, X_{SRB}	0.006	g S/g COD_X
$i_{S,XB}$	Sulfur content of slowly biodegradable COD, X_B	0.000	g S/g COD_X
$i_{S,I}$	Sulfur content of particulate inert COD, X_I	0.000	g S/g COD_X
Stoichiometric:			
$f_{I,H}$	Fraction of particulate inert COD by X_H decay	0.10	g COD_X /g COD_X
f_{I,SeO_4}	Fraction of particulate inert COD by X_{SeO_4} decay	0.10	g COD_X /g COD_X
f_{I,SeO_3}	Fraction of particulate inert COD by X_{SeO_3} decay	0.10	g COD_X /g COD_X
$f_{I,SRB}$	Fraction of particulate inert COD by X_{SRB} decay	0.10	g COD_X /g COD_X

concentration is 1 g Se/m^3, then a maximum 1.9% of the selenium removal can be achieved by assimilation into denitrifying heterotrophic bacteria. Hence, sufficient removal of selenium oxyanions by assimilation for synthesis of denitrifying heterotrophs can be feasible only when the N:Se ratio is very much greater than 50 g N:1 g Se. Thus, we conclude that a substantial removal of selenium oxyanions can occur only through their respiration.

4.4 MINIMUM SRT AND DONOR-SUBSTRATE CONCENTRATION

A reliable diagnostic parameter is the minimum solids residence time ($SRT_{\text{lim}}^{\text{min}}$) required to accumulate steady-state biomass. It can be calculated by:

$$SRT_{\text{lim}}^{\text{min},k} = \frac{1}{\mu_{\text{max},k} - b_k} \tag{4.15}$$

The minimum solids residence time (*SRT*) tells us how long the actual *SRT* must be to avoid the washout of a biomass *k*. Reliable performance requires an actual *SRT* that is greater than the minimum value calculated using Equation (4.15). A comparison of the actual *SRT* to the minimum *SRT* applies equally to suspended-growth and biofilm processes, although the method to compute the actual *SRT* differs (Rittmann & McCarty, 2020). As *SRT* increases well above the minimum *SRT*, the concentration of S_i approaches a limiting value that represents the minimum concentration of substrate *i* that is capable of supporting steady-state biomass ($S_{\text{min},i}$). $S_{\text{min},i}$ can be calculated by:

$$S_{\text{min},i} = K_i \frac{b_k}{\mu_{\text{max},k} - b_k} \tag{4.16}$$

Here, K_i is the half-saturation concentration of substrate *i* (g/m^3), which can be the electron donor or acceptor, depending on which one is rate-limiting.

Applying Equations (4.15) and (4.16), along with the appropriate $\mu_{\text{max},k}$, b_k, and K_i parameter values listed in Table 4.7, makes it possible to compute $SRT_{\text{lim}}^{\text{min},k}$ and $S_{\text{min},i}$ for the electron acceptor and donor used by each bacterial group considered. These values are listed in Table 4.9 and provide two very important insights into anaerobic bioreactors exposed to wastewater containing nitrate, selenate/selenite, and sulfate. First, all of the $S_{\text{min},i}$ values are much less than 1 g/m^3, and the values for selenate and selenite are less than 0.0001 g/m^3. This means that a biological process with a long-enough SRT can drive the concentrations of all oxyanions, as well as acetate, to very low concentrations. Second, the $SRT_{\text{lim}}^{\text{min}}$ values span a large range. For example, the $SRT_{\text{lim}}^{\text{min}}$ for sulfate-reducing bacteria is nearly 14-fold greater than that for denitrifying heterotrophic bacteria. Likewise, the bacteria respiring selenium oxyanions have $SRT_{\text{lim}}^{\text{min}}$ values that are

Table 4.9 Comparison of estimated $SRT_{lim,i}^{min,k}$ and $S_{min,i}$ values for the four types of respiration.

Variable	Symbol	$SRT_{lim,i}^{min,k}$ (days)	$S_{min,i}$ (g/m^3)
1. Minimum *SRT*, Denitrifying heterotrophic bacteria	X_H	0.10	
2. Concentration at a long *SRT*			
a. Nitrate	S_{NO_3}		0.02
b. Acetate	S_{VFA}		0.16
3. Minimum *SRT*, Selenate-reducing bacteria	X_{SeO_4}	0.14	
4. Concentration at a long *SRT*			
a. Selenate	S_{SeO_4}		0.00004
b. Acetate	S_{VFA}		0.16
5. Minimum *SRT*, Selenite-reducing bacteria	X_{SeO_4}	0.19	
6. Concentration at a long *SRT*			
a. Selenite	S_{SeO_3}		0.00004
b. Acetate	S_{VFA}		0.16
7. Minimum *SRT*, Sulfate-reducing bacteria	X_{SRB}	1.38	
8. Concentration at a long *SRT*			
a. Sulfate	S_{SO_4}		0.01
b. Acetate	S_{VFA}		0.16

7 to 10-fold less than that for sulfate-reducing bacteria. These differences mean that – at least in principle – sulfate-reduction can be suppressed or minimized by selecting an operating *SRT* that supports the accumulation of denitrifying heterotrophic bacteria and SeRB, but prevents the accumulation of sulfate-reducing bacteria.

4.5 SIMULATION OF SeRB POPULATION DYNAMICS

We carried out simulations using a commercially available wastewater treatment plant simulator (SUMO®, Dynamita, France). In both cases, a continuous flow stirred tank reactor (CFSTR) was modeled which has a hydraulic retention time (*HRT*) equal to the *SRT*.

4.5.1 Model comparison with observed selenium oxyanion reduction

A focused evaluation of our SeRB model was carried out by simulating the experimental system reported by Fujita *et al.* (2002) and then comparing the model output with data reported by the researchers. They operated a

laboratory-scale CFSTR ($V_R = 0.0005\ m^3$) inoculated with SeRB. The CFSTR was fed synthetic wastewater having concentrations of 42 g Se/m^3 as selenate and 2200 g COD/m^3 as lactate. The influent flow rate was adjusted to achieve SRT values of 2.9, 6.0, 8.9, 12.0, 23.8, 48.0, and 95.2 hours. A biomass concentration of 28.4 g COD_X/m^3 in the CFSTR was reported by Fujita *et al.* (2002).

Since lactate was the electron donor instead of acetate, the energy equation should consider lactate ($CH_3CHOHCOO^-$) as the common electron donor for the electron acceptors selenate and selenite. Equation (4.17) is the half reaction for lactate reduction and its free energy (Rittmann & McCarty, 2020).

$$\frac{1}{12}CH_3CHOHCOO^- + \frac{1}{3}H_2O \rightarrow \frac{1}{6}CO_2 + \frac{1}{12}HCO_3^- + H^+ + e^-$$
$$\Delta G^{0'}_{ED} = +32.3\frac{kJ}{e^-eq_{ED}} \tag{4.17}$$

Combining Equations (4.2) and (4.17) and combining Equations (4.3) and (4.17) result in the energy reactions for selenate and selenite reduction, respectively, when lactate is the common electron donor (Equations (4.18) and (4.19)). Also shown are the free energy values for each energy reaction ($\Delta G^{0'}$) in kJ/e^-eq.

$$\frac{1}{12}CH_3CHOHCOO^- + \frac{1}{2}SeO_4^{2-} + \frac{1}{2}H^+ \rightarrow \frac{1}{12}CO_2 + \frac{1}{2}HSeO_3^- + \frac{1}{12}HCO_3^- + \frac{5}{24}H_2O \quad \Delta G^{0'}_{ED} = -76.2\frac{kJ}{e^-eq_{ED}} \tag{4.18}$$

$$\frac{1}{12}CH_3CHOHCOO^- + \frac{1}{4}HSeO_3^- + \frac{1}{4}H^+ \rightarrow \frac{1}{12}CO_2 + \frac{1}{4}Se^0 + \frac{1}{12}HCO_3^- + \frac{5}{25}H_2O \quad \Delta G^{0'}_{ED} = -57.7\frac{kJ}{e^-eq_{ED}} \tag{4.19}$$

Applying Equations (4.10) through (4.14), the following parameter values were calculated for:

(1) Selenate-reducing bacteria:
- $Y_{SeO_4,lactate} = 0.58$ g COD_X/g COD_{ED}
- $\hat{q}_{SeO_4,lactate} = 13.5$ g COD_{ED}/(g $COD_X \cdot$ d)
- $\mu_{SeO_4,lactate} = 7.9$ 1/d

(2) Selenite-reducing bacteria:
- $Y_{SeO_3,lactate} = 0.51$ g COD_X/g COD_{ED}
- $\hat{q}_{SeO_3,lactate} = 11.6$ g COD_{ED}/(g $COD_X \cdot$ d)
- $\mu_{SeO_3,lactate} = 6.0$ 1/d

Based on these parameter values, Figure 4.3 presents the selenate, selenite, and elemental selenium concentrations observed by Fujita *et al.* (2002) and those

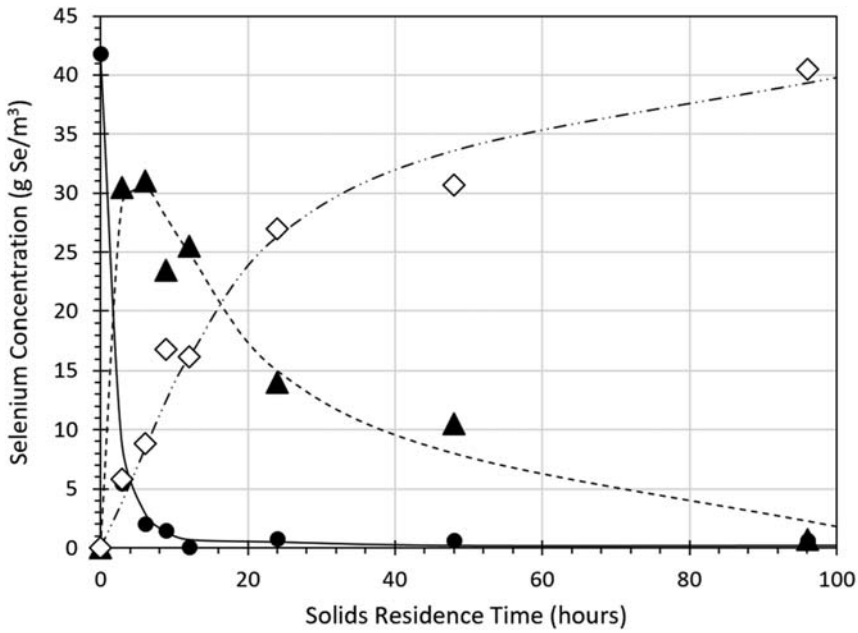

Figure 4.3 Observed selenate (●), selenite (▲), and elemental selenium (◇) concentrations in the effluent of a bench-scale continuous-flow stirred-tank reactor (CFSTR) versus solids residence time. Data reported by Fujita *et al.* (2002). Observations compared to simulated selenate (—), selenite (----), and elemental selenium (–···–) concentrations.

resulting from the simulation of their experimental system using the SeRB model described in this chapter (i.e., neglecting denitrifying heterotrophic and sulfate-reducing bacteria). The experimental data and model results agree well in terms of all trends and absolute concentrations, and the coefficients of determination (R^2) for selenate, selenite, and elemental selenium are 0.99, 0.97, and 0.97, respectively. The observed rate of selenium-oxyanion ($S_{SeO_4} + S_{SeO_3}$) reduction was 0.37 g Se/g $COD_x \cdot$ d, which is similar to the simulated selenium-oxyanion reduction rate of 0.35 g Se/g $COD_x \cdot$ d.

4.5.2 Ecology of denitrifying heterotrophic bacteria, selenium-respiring bacteria, and sulfate-reducing bacteria

To evaluate the microbial ecology of a reactor treating wastewater containing typical concentrations of nitrate, selenate, and sulfate, we simulated a 1 m^3 CFSTR. The simulated influent concentration of nitrate was 50 g N/m^3, selenate was 1 g Se/m^3, and sulfate was 1000 g S/m^3. The simulated wastewater flow rate was adjusted to give SRTs that were incrementally increased from 0 to 8.5 days. Each

simulated wastewater flow rate equals the CFSTR volume (1 m^3) multiplied by the *SRT*. Initially, we used influent electron donor, macro- and micro-nutrient concentrations that were non-rate limiting: acetate was 3000 g COD/m^3, ammonium was 100 g N/m^3, hydrogen sulfide was 1 g S/m^3, and hydrogen selenide was 0.1 g Se/m^3. Subsequently we lowered the influent electron donor concentration to 500 g COD/m^3, while the other essential nutrient concentrations remained the same.

Figure 4.4 illustrates acetate (as COD), nitrate (as N), selenate (as Se), selenite (as Se), elemental selenium (as Se), sulfate (as S), and hydrogen sulfide (as S) as a function of SRT. The first thing to notice is that the effluent contains a significant concentration of acetate (at least 500 g COD/m^3) because the simulations were set up with an acetate-input concentration greater than what is needed for the stoichiometric reduction of all oxyanions. This approach emphasizes the relative specific growth rates impacts, but not competition for the electron donor (i.e., acetate).

Figure 4.4 shows significant nitrate reduction to 0.20 g N/m^3, after a 0.4-day *SRT*, which is greater than its $SRT_{\lim}^{\min,H}$ of 0.10 days. The simulated nitrate concentration for *SRTs* greater than 0.4 days approaches the $S_{\min,NO_3}$ value 0.02 g N/m^3. Similarly, Figure 4.4 illustrates significant selenate reduction to 0.0075 g Se/m^3 after a 1.5-day *SRT*, which is greater than its $SRT_{\lim}^{\min,SeO_4}$ of 0.14 days. When the *SRT* is greater than 1.5 days, the effluent selenate concentration approaches its $S_{\min,SeO_4}$ value of 0.00004 g Se/m^3. For selenite, Figure 4.4 illustrates its significant reduction to 0.0093 g Se/m^3 after a 4.0-day *SRT*, which is greater than its $SRT_{\lim}^{\min,SeO_3}$ of 0.19 days. For *SRTs* greater than 4.0 days, the selenite concentration approaches its $S_{\min,SeO_3}$ value of 0.00004 g Se/m^3. Finally, Figure 4.4 illustrates that sulfate reduction begins when the *SRT* is around 2.0 days, which is greater than its $SRT_{\lim}^{\min,SRB}$ of 1.38 days. Significant sulfate reduction, to 0.28 g S/m^3, occurs at an 8.5-day *SRT*. These results illustrate the generalizable trend that the actual *SRT* must be roughly three-fold greater than $SRT_{\lim}^{\min,k}$ to drive the concentration of substrate *i* to low levels.

Reducing the influent acetate concentration to a value that is substantially less than what is required to stoichiometrically convert all of the oxyanions to their most reduced state has a profound impact on simulation results. Figure 4.5 shows the effects of lessening the influent acetate concentration to 500 g COD/m^3, which provides only 17% of the stoichiometric demand to reduce all of the oxyanions. While denitrification, selenate reduction, and selenite reduction are hardly affected, sulfate reduction is almost entirely suppressed. Because sulfate-reducing bacteria are the slowest growing bacteria, they can be out-competed for acetate if its supply cannot meet the demand of all oxyanions. In this example, sulfate has the greatest electron-donor demand, which means that only 17% of the electron donor needed for all oxyanions was sufficient for the reduction of nitrate, selenate, and selenite.

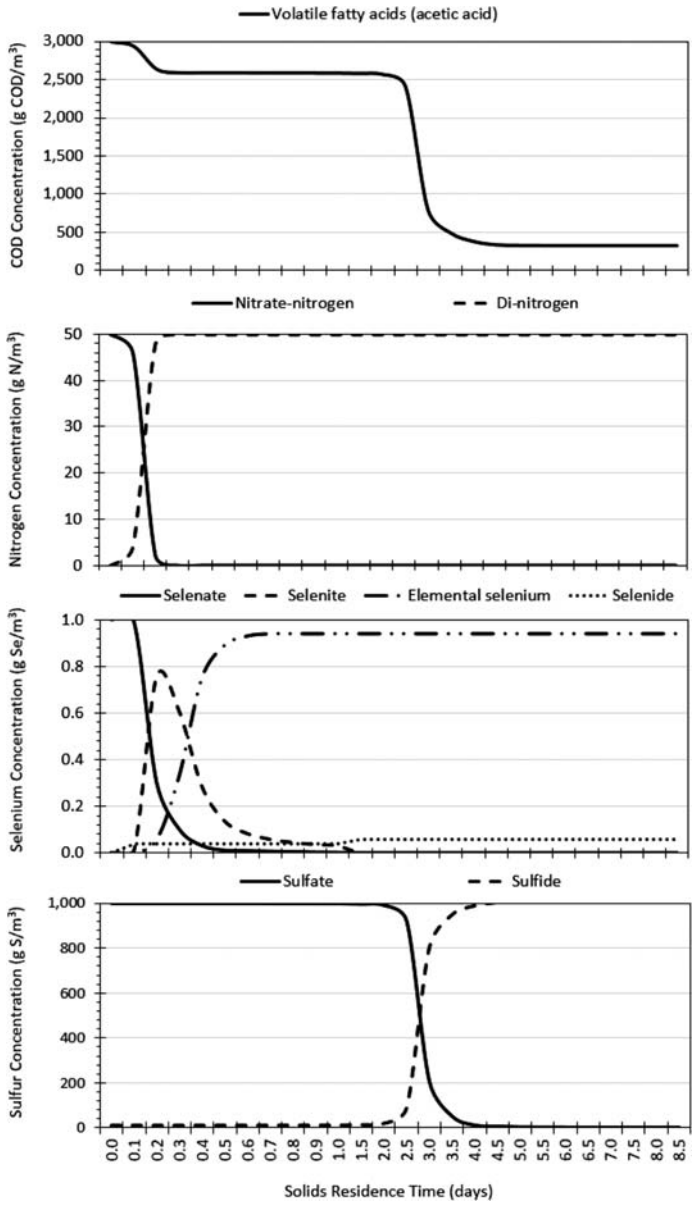

Figure 4.4 Impact of *SRT* on acetate, nitrate, selenate, selenite, elemental selenium, hydrogen selenide, sulfate, and hydrogen sulfide concentrations in a continuous-flow stirred-tank reactor (CFSTR) treating wastewater containing concentrations of acetate = 3000 g COD/m^3, nitrate = 50 g N/m^3, selenate = 1 g Se/m^3, and sulfate = 1000 g S/m^3.

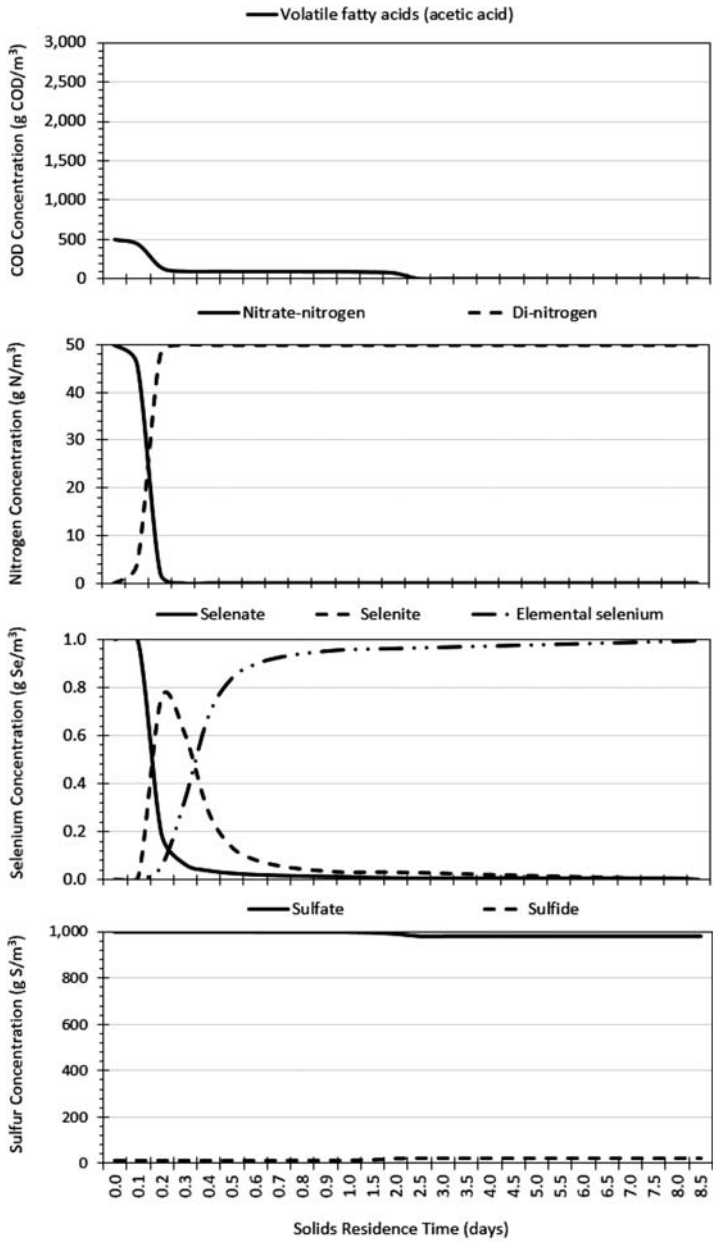

Figure 4.5 Impact of *SRT* on acetate, nitrate, selenate, selenite, elemental selenium, sulfate, and hydrogen sulfide concentrations in a continuous-flow stirred-tank reactor (CFSTR) treating wastewater containing concentrations of acetate = 500 g COD/m^3, nitrate = 50 g N/m^3, selenate = 1 g Se/m^3, and sulfate = 1000 g S/m^3.

4.6 KEY POINTS

- The thermodynamics of the respiration reactions, manifested with values of Y_k and $\mu_{\max,k}$ give major growth advantages in the order: denitrification > selenate reduction > selenite reduction > sulfate reduction.
- As sulfate reduction normally is undesired, it can be suppressed by maintaining a sufficiently short *SRT*, controlling the electron-donor supply, or a combination thereof.
- In contrast, using a too long *SRT* with a too great input of electron donor will allow sulfate reduction.
- Using a too low *SRT* also can suppress selenite reduction, even if selenate reduction occurs.

REFERENCES

Boltz J. P. and Rittmann B. E. (2019). A model of Selenium, Sulfur, and Nitrogen Species (SeSANS) conversion in a biofilm reactor. EPRI, Palo Alto, CA. 3002017266.

De Souza M. P., Amini A., Dojka M. A., Pickering I. J., Dawson S. C., Pace N. R. and Terry N. (2001). Identification and characterization of bacteria in a selenium-contaminated hypersaline evaporation pond. *Applied and Environmental Microbiology*, **67**(9), 3785–3794.

EPA (2020). Steam electric reconsideration rule. 40 CFR Part 23; 6560-50-P. RIN 2040-AF77.

Eswayah A. S., Smith T. J. and Gardiner P. H. E. (2016). Microbial transformations of selenium species of relevance to bioremediation. *Applied and Environmental Microbiology*, **82**(16), 4848–4859.

Fujita M., Ike M., Kashiwa M., Hashimoto R. and Soda S. (2002). Laboratory-scale continuous reactor for soluble selenium removal using selenate-reducing bacterium, *Bacillus* sp. SF-1. *Biotechnology and Bioengineering*, **80**(7), 755–761.

Grady C. P., Daigger G. T., Love N. G. and Filipe C. D. M. (2011). Biological wastewater treatment, 3rd edn, IWA Publishing, CRC Press, Boca Raton, FL.

Macy J. M., Lawson S. and Decker H. D. (1993). Bioremediation of selenium oxyanions in San Joaquin drainage water using *Thauera selenatis* in a biological reactor system. *Applied Microbiology and Biotechnology*, **40**, 588–594.

McCarty P. L. (2007). Thermodynamic electron equivalents model for bacterial yield prediction: modifications and comparative evaluations. *Biotechnology and Bioengineering*, **97**(2), 377–388.

Mörschbächer A. P., Dullius A., Dullius C. H., Bandt C. R., Kuhn D., Brietzke D. T., Kuffel F. J. M., Etgeton H. P., Altmayer T., Gonçalves T. E., Oreste E. Q., Ribeiro A. S., de Souza C. F. V. and Hoehne L. (2018). Validation of an analytical method for the quantitative determination of selenium in bacterial biomass by ultraviolet-visible spectrophotometry. *Food Chemistry*, **255**(30), 1820186.

Olin Å., Noläng B., Osadchii E. G., Öhman L.-O. and Rosén E. (2020). Chemical thermodynamics of selenium. OECD Nuclear Energy Agency, Data Bank.

PSI (Paul Scherrer Institute) (2007). The PSI/Nagra chemical thermodynamic database: data selection of selenium. TM-44-14-07.

Rittmann B. E. and McCarty P. L. (2020). *Environmental Biotechnology: Principles and Applications*, 2nd edn, McGraw-Hill, U.S.A.

Switzer Blum J., Burns Bindi A., Buzzelli J., Stolz J. F. and Oremland R. S. (1998). *Bacillus arsenicoselenatis*, sp. nov., and *Bacillus selenitireducens*, sp. nov.: two haloalkaliphiles from Mono Lake, California that respire oxyanions of selenium and arsenic. *Archives of Microbiology*, **171**, 19–30.

Tan L. C. (2018). Anaerobic treatment of mine wastewater for the removal of selenate and its co-contaminants. Doctoral dissertation. Université Paris-est and UNESCO-IHE.